Electronic Journal of Biotechnology 67 (2024) 13–22

Contents lists available at ScienceDirect

Electronic Journal of Biotechnology

journal homepage: www.elsevier.com/locate/ejbt

Research article

Unraveling SARS-CoV-2-associated lncRNAs' prognostic significance in lung adenocarcinoma-survival, immunity, and chemotherapy responses ☆

Qianhui Zhou [a], Ting Yuan [a], Zhimin Xie [b], Ying Chen [a,c,*]

[a] Department of Respiratory and Critical Care Medicine, Zhuzhou Central Hospital, Zhuzhou 412000, Hunan, China
[b] Department of Stomatology, Zhuzhou Central Hospital, Zhuzhou 412000, Hunan, China
[c] Department of Childcare, Changsha Hospital for Maternal and Child Health Care Affiliated to Hunan Normal University, ChangSha 410007, Hunan, China

GRAPHICAL ABSTRACT

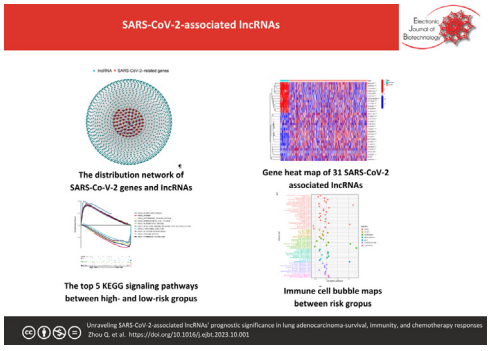

ARTICLE INFO

Article history:
Received 2 August 2023
Accepted 5 October 2023
Available online 29 October 2023

Keywords:
Clinical prognosis
COVID-19
Drug sensitivity
Immune function
lncRNA
Lung adenocarcinoma
Lung cancer
Molecular biomarkers
Prognostic risk model
SARS-CoV-2
Therapeutic targets

ABSTRACT

Background: This study investigates the link between SARS-CoV-2-associated long non-coding RNAs (lncRNAs) and lung adenocarcinoma (LUAD). LUAD is a prevalent and aggressive lung cancer type. The study aims to identify prognostic lncRNAs and construct a predictive model while shedding light on potential therapeutic targets during the COVID-19 era.
Results: Eight SARS-CoV-2-associated lncRNAs with significant prognostic value in LUAD were identified, forming a robust prognostic risk model. The model exhibited strong predictive performance, with high area under the ROC curve (AUC) values at one, three, and five years. Furthermore, the risk score was an independent prognostic factor, correlating with the cancer stage. Notably, differences in immune function, drug sensitivity, and immune checkpoint expression were observed between high- and low-risk groups.
Conclusions: This study unveils eight SARS-CoV-2-associated lncRNAs as valuable prognostic markers in LUAD, yielding a reliable prognostic risk model. Additionally, the model's ability to predict patient outcomes and its correlation with cancer stage underscores its clinical utility. The observed variances in immune function, drug sensitivity, and immune checkpoint expression suggest potential avenues for personalized LUAD treatment strategies. Clinicians can utilize the prognostic risk model to predict LUAD patient outcomes, informing treatment decisions. The insights into immune function, drug sensitivity, and immune checkpoints offer opportunities for tailored therapies, potentially enhancing patient

Peer review under responsibility of Pontificia Universidad Católica de Valparaíso
☆ Audio abstract available in Supplementary material.
* Corresponding author.
E-mail address: chenying111594@126.com (Y. Chen).

https://doi.org/10.1016/j.ejbt.2023.10.001

outcomes. This study underscores the importance of considering the interplay between SARS-CoV-2-associated factors and cancer biology, especially in the context of the COVID-19 pandemic.
How to cite: Zhou Q, Yuan T, Xie Z, et al. Unraveling SARS-CoV-2-associated lncRNAs' prognostic significance in lung adenocarcinoma-survival, immunity, and chemotherapy responses. Electron J Biotechnol 2024;67. https://doi.org/10.1016/j.ejbt.2023.10.001.

1. Introduction

Lung cancer is the most prevalent malignant tumor worldwide, with an average of about 2,100 people being diagnosed with lung cancer every day [1]. Lung adenocarcinoma (LUAD) is a pathological type of lung cancer. Hematological metastasis occurs at the early stage of LUAD, while lymphatic metastasis usually occurs at the advanced stage [2]. Although molecular targeted therapies improve the overall survival (OS) of LUAD to a certain extent [3], it is only effective in a few patients, and the cost is high. Therefore, seeking more comprehensive clinical therapeutic targets is beneficial to improve the OS rate of LUAD patients.

There was an onset of widespread infection of a β-coronavirus called the novel coronavirus (SARS-CoV-2) in the South China Seafood Market, Wuhan, Hubei Province in late December 2019 [4,5]. Following SARS-CoV and MERS-CoV, SARS-CoV-2 is a highly pathogenic coronavirus, which has been reported to cause severe respiratory diseases that might lead to death in humans [6]. Many studies have found that cancer patients are more likely to develop severe pneumonia after a SARS-COV-2 infection. Similarly, multiple mediators secreted by COVID-19 affect tumor progression by altering the tumor microenvironment [7,8]. SARS-CoV-2 encodes for four different structural proteins: membrane (M), envelope (E), spike (S), and nucleocapsid (N) [9]. Receptor-binding domain (RBD) of the spike protein (S) interacts with angiotensin-converting enzyme 2 (ACE2), thereby facilitating the transmission of the virus within humans and across different species [10].

Long noncoding RNA (LncRNAs) are encoded by the genome, most of which do not translate into proteins but play a major role in gene regulation [11]. A study has confirmed that lncRNA participates in the biological behavior of tumors [12]. To date, SARS-CoV-2-associated lncRNAs have not been reported to be associated with LUAD. The current study aimed to develop a predictive model of SARS-CoV-2-associated lncRNAs based on the TCGA database and analyzed its function enrichment and immune-related function to explore its possible mechanism.

2. Materials and methods

2.1. Data collection and collation

The mRNA transcripts and clinical data associated with a total of 501 LUAD and 54 control tissue samples were retrieved from the Cancer Genome Atlas (TCGA) database. Samples with short survival and incomplete clinical data were excluded. Ultimately, 468 LUAD samples were included in the final analysis, where the "Caret" package of the R software was used to randomize the data set into a training set (N = 236) and a testing set (N = 235). A total of 333 SARS-CoV-2-associated genes were extracted from the Human Protein Atlas (HAP) database. A total of 1385 SARS-CoV-2-associated lncRNAs were screened using Pearson correlation calculation. In addition, we extracted 767 differentially expressed SARS-CoV-2-associated lncRNAs using the "Limma" package of the R software. We observed differentially expressed lncRNAs and genes associated with SARS-CoV-2 using the "GGPLOT2" package of the R software.

2.2. A prognostic risk model based on SARS-CoV-2-associated lncRNAs in LUAD

Univariate Cox regression, multivariate Cox regression, and LASSO analyses were performed on the training set using "Survival" and "Glmnet" packages of the R software [13,14]. We identified 8 SARS-CoV-2-associated lncRNAs linked to survival in LUAD patients and then used them to construct the lncRNAs model. Lasso regression was used to fit the generalized linear model of data with variable selection and complexity adjustment, and the degree of complexity adjustment was controlled by the parameter λ to avoid over-fitting. Expression levels of lncRNAs and the corresponding regression coefficient were used to calculate the risk score (RS) for each sample with Equation 1:

$$RS = \sum_{k=1}^{n} coef\left(lncRNA^{k}\right) * expr\left(lncRNA^{k}\right) \quad \text{(Equation1)}$$

Depending on their median RS values, patients in the testing, training, and entire sets were categorized into the high- and low-risk groups.

2.3. Assessment and validation of the predictive performance of the SARS-CoV-2-associated lncRNAs prognostic risk model

To thoroughly test the predictive performance of the SARS-CoV-2-associated lncRNAs prognostic risk model, the training, testing, and entire sets were analyzed using the "Time Roc" package of the R software [15,16]. The RS, survival status, overall survival, and lncRNA distribution were analyzed. Further, ROC analysis, a tool for describing the accuracy of diagnostic tests or predictive models, was performed. The AUC were compared to evaluate the model. Subsequently, the SARS-CoV-2-associated lncRNAs model and the respective data for clinical pathology were used to determine their independence using univariate and multivariate Cox regression analyses for the above three sets. Finally, the Kaplan-Meier curve was generated to visualize the differences in age, sex, and tumor stage between the groups.

2.4. Principal component analysis (PCA)

PCA serves as a method for statistical analysis and simplification of datasets. Furthermore, SARS-CoV-2-associated genes and lncRNAs and the number of genes in the model were reduced to three dimensions and plotted using "Limma" and "Scatterplot 3D" packages of R software [15,16].

2.5. Nomogram and calibration

A nomogram was developed to predict one-, three-, and five-year survival in patients with LUAD using the RMS software package based on multivariate Cox regression analysis of RS and clinicopathological data of the entire set. In addition, we used the "Survival Roc" package to test the predictive performance of the nomogram. Subsequently, the calibration curve was further drawn to evaluate the accuracy of the nomogram results and to validate its performance.

2.6. Pathway enrichment analysis and immune-related function research

The differences in tumor-infiltrating immune cell subsets, immune microenvironment, and immune checkpoint between the high- and low-risk groups were evaluated using GSEA analysis to understand the pathways enriched in the SARS-CoV-2-associated LncRNAs model in the two groups. In addition, we evaluated the immune cell components of the two groups by the ssGSEA algorithm.

2.7. Analysis of the predictive value of the risk model in therapeutic strategies of LUAD

IC50 is an important factor in evaluating the drug efficacy or sample treatment response. The sensitivity of LUAD patients to anti-tumor drugs between the two groups was analyzed by the r-package "p-RRophetic" package of the R software.

3. Results

3.1. Extraction of SARS-CoV-2-associated lncRNAs

The study design is demonstrated in Fig. 1. The differential expression among 767 SARS-CoV-2-associated lncRNAs was analyzed in 501 LUAD tissues and 54 control tissues in the TCGA cohort (log FC (fold change) > 1.0, FDR (false discovery rate) < 0.05). A volcano plot of SARS-CoV-2-associated lncRNAs is shown in Fig. 2A, where red dots represent 670 highly expressed SARS-CoV-2-associated lncRNAs and green dots represent 97 low-expressed SARS-CoV-2-associated lncRNAs. The network relationship between SARS-CoV-2-associated lncRNAs and genes is shown in Fig. 2B.

3.2. Construction of SARS-CoV-2-associated lncRNAs prognostic risk model

Patients in the entire set (N = 468) were randomly divided in a 1:1 ratio into the testing set (N = 234) and the training set

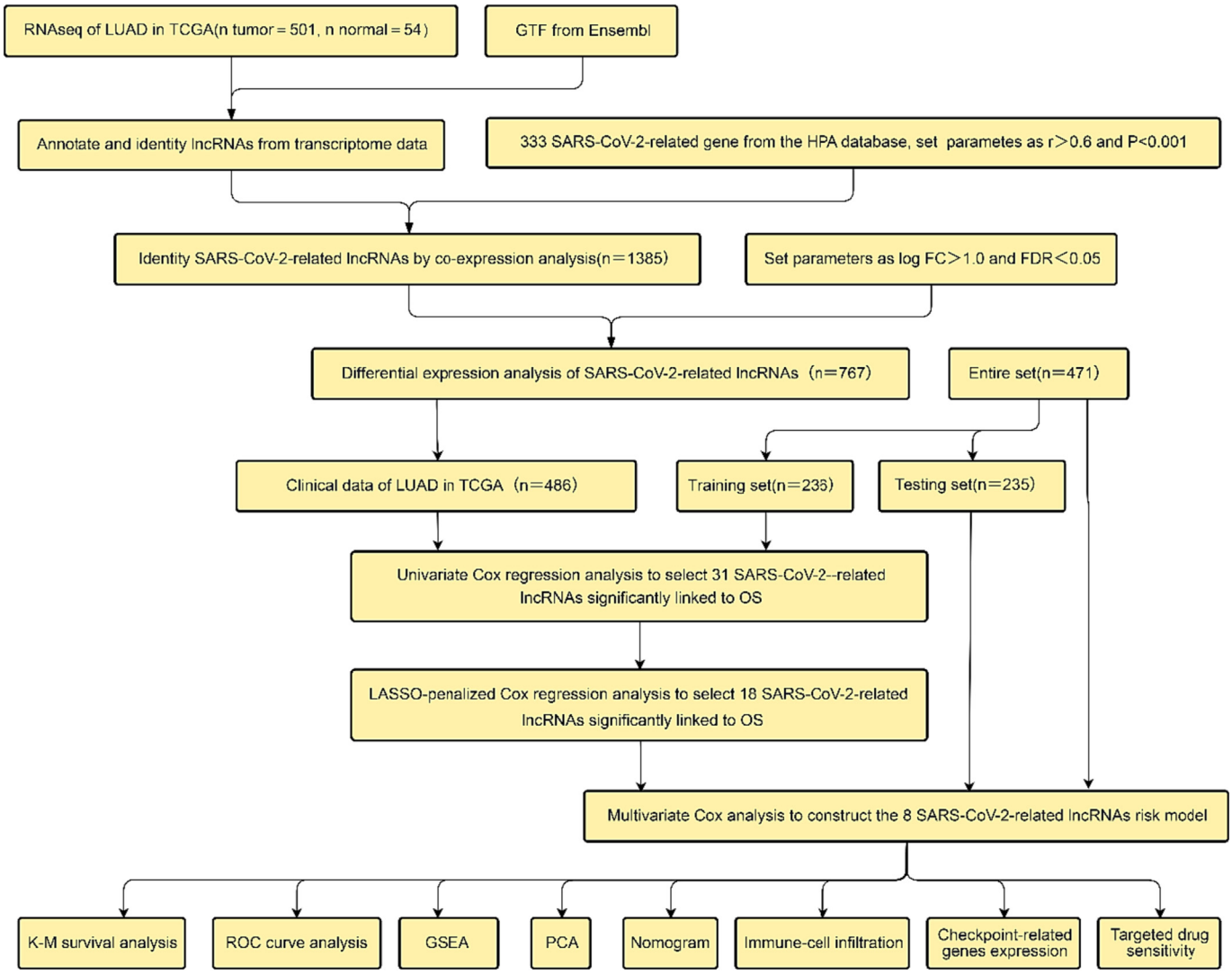

Fig. 1. The flow chart demonstrates the data collection and analysis used in this study.

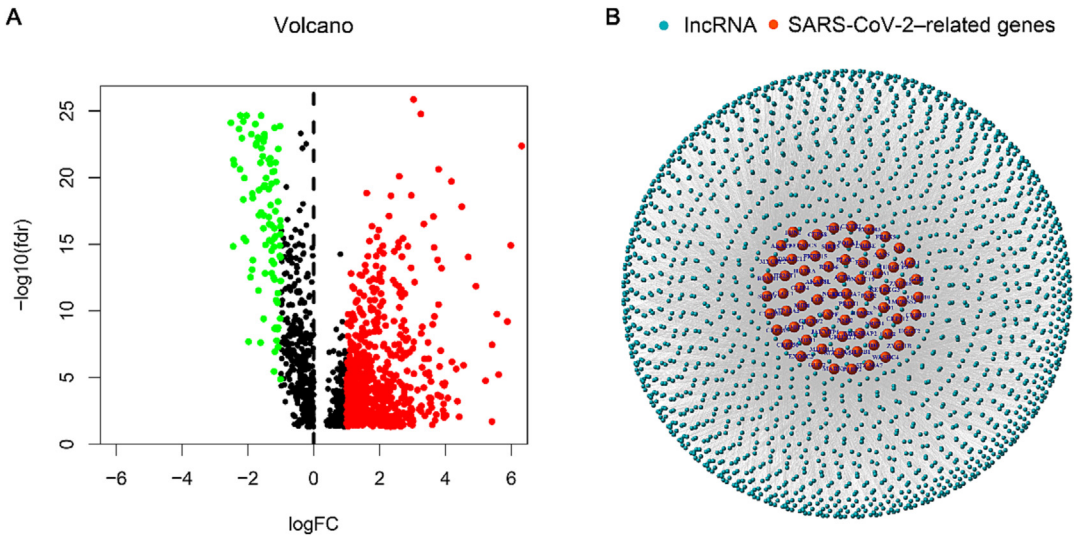

Fig. 2. SARS-CoV-2-associated lncRNAs were extracted from LUAD patients. (A) Volcanic map of SARS-CoV2 related lncRNA downregulated and upregulated differential expression. (B) The distribution network of SARS-CoV-2 genes and lncRNAs.

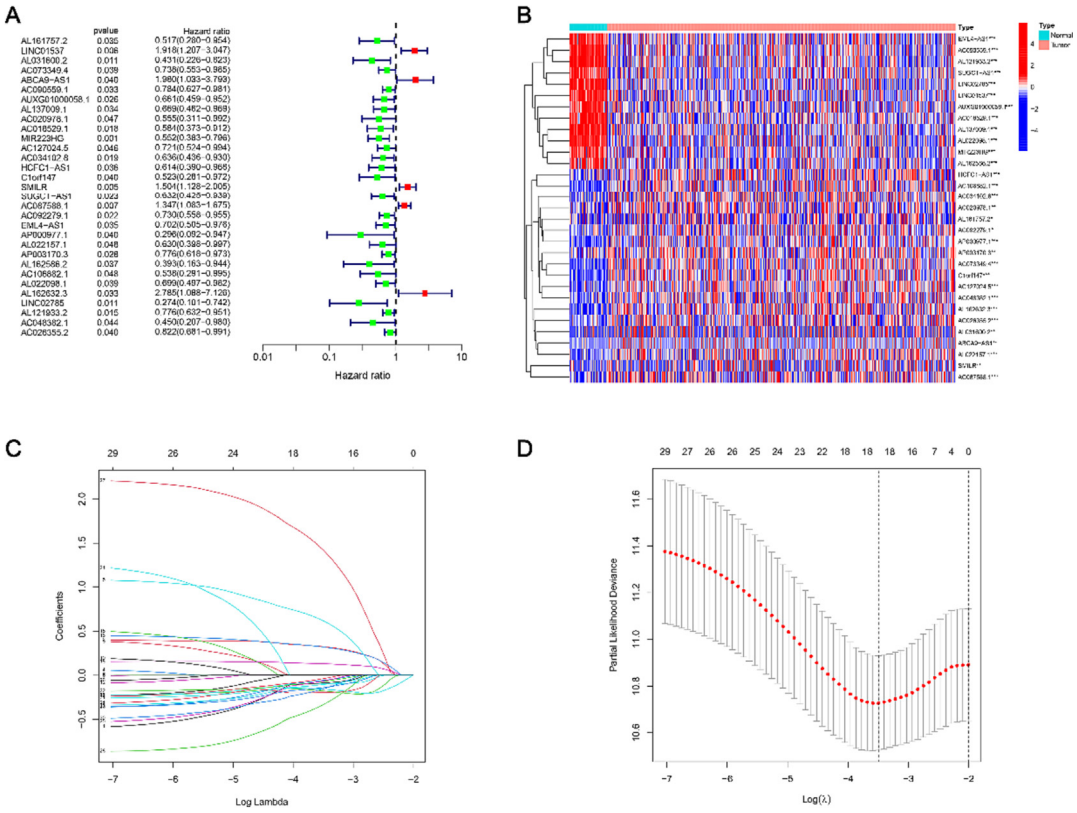

Fig. 3. Construction of SARS-CoV-2-associated lncRNAs prognostic model in LUAD. (A) Univariate Cox regression analysis screened SARS-CoV-2-associated lncRNAs and plotted forest plots. (B) Gene heat map of 31 SARS-CoV-2-associated lncRNAs. (C) Lasso regression of SARS-CoV-2-associated lncRNA model based on Lambda. (D) Lasso regression coefficient curves of 18 SARS-CoV-2-associated lncRNAs.

(N = 234). In the training set, univariate Cox regression identified 31 SARS-CoV-2-associated lncRNAs related to the survival of LUAD patients ($p < 0.05$) (Fig. 3A). The distribution of 31 lncRNAs between tumor and normal tissue samples was demonstrated using a heat map (Fig. 3B). To avoid over-fitting, we further performed LASSO regression analysis to de-dimensionalize the data and extracted 18 SARS-CoV-2-associated lncRNAs (Fig. 3C,D). Finally, multivariate COX regression analysis identified a total of 8 SARS-CoV-2-associated lncRNAs as prognostic factors in LUAD patients.

3.3. Validation of SARS-CoV-2-associated lncRNAs prognostic risk model

To verify the predictive performance of the risk model, we analyzed the training, testing, and entire sets. First, the difference in survival between the two groups was analyzed. The RS chart, survival status chart, risk heatmap, and K-M survival curve demonstrated a gradual increase in the mortality of the patients with an increase in RS (Fig. 4). The OS of the low-risk group was significantly higher than the high-risk group ($p < 0.001$). RS has a

significant effect on the prognosis of patients diagnosed with LUAD. Then, the AUC values of the one-, three- and five-year survival were calculated to be 0.741, 0.744, and 0.755 for the training set, respectively (Fig. 5A), 0.715, 0.610, and 0.617 for the testing set, respectively (Fig. 5B), and 0.729, 0.677, and 0.677 for the entire set, respectively (Fig. 5C).

These results indicated that the model could effectively predict survival. Finally, univariate and multivariate Cox retrospective independent prognostic analyses of RS and clinical data (age, sex, tumor stage) were performed to understand the clinical significance of the prognostic model. Univariate Cox regression identified tumor stage, T stage, N stage, and RS to be independent prognostic indicators in the training set (Fig. 5D), whereas multivariate independent prognostic analysis identified N stage and RS to be independent prognostic factors in LUAD patients (Fig. 5E). In the testing set, univariate Cox regression identified tumor stage, T stage, N stage, M stage, and RS to be independent prognostic indicators (Fig. 5F), whereas multivariate independent prognostic analysis identified RS to be an independent prognostic factor in LUAD patients (Fig. 5G). In the entire set, univariate Cox regression identified tumor stage, T stage, N stage, M stage, and RS to be independent prognostic indicators (Fig. 5H), whereas multivariate independent prognostic analysis identified RS to be an independent prognostic factor in LUAD patients (Fig. 5I). The results of univariate and multivariate COX regression analyses identified RS as an independent prognostic factor in LUAD patients as it was independent of other clinical factors. Kaplan-Meier analyses of patients' OS based on T stage, N stage, M stage, age, and sex demonstrated that patients with low-risk scores had longer survival period (Fig. 6). The above results further confirmed the reliability of the model in predicting prognosis.

3.4. PCA verified the predictive performance of the model

Based on the samples of low- and high-risk groups, the genome-wide, SARS-CoV-2-associated genes, SARS-CoV-2-associated lncRNAs, and SARS-CoV-2-associated lncRNAs prognostic risk model were analyzed by PCA. These genes and lncRNAs are likely identified based on their known interactions with the virus or their differential expression in response to SARS-CoV-2 infection. The SARS-CoV-2-associated lncRNAs model refers to the constructed prognostic risk model based on the selected SARS-CoV-2-associated lncRNAs. As shown in Fig. 7A-D, using genome-wide or SARS-CoV-2-associated lncRNAs cannot effectively distinguish high- and low-risk populations. However, using the SARS-CoV-2-associated lncRNAs model can accurately distinguish patients with different risk scores, further verifying the model's predictive effectiveness. These results indicate that the SARS-CoV-2-associated

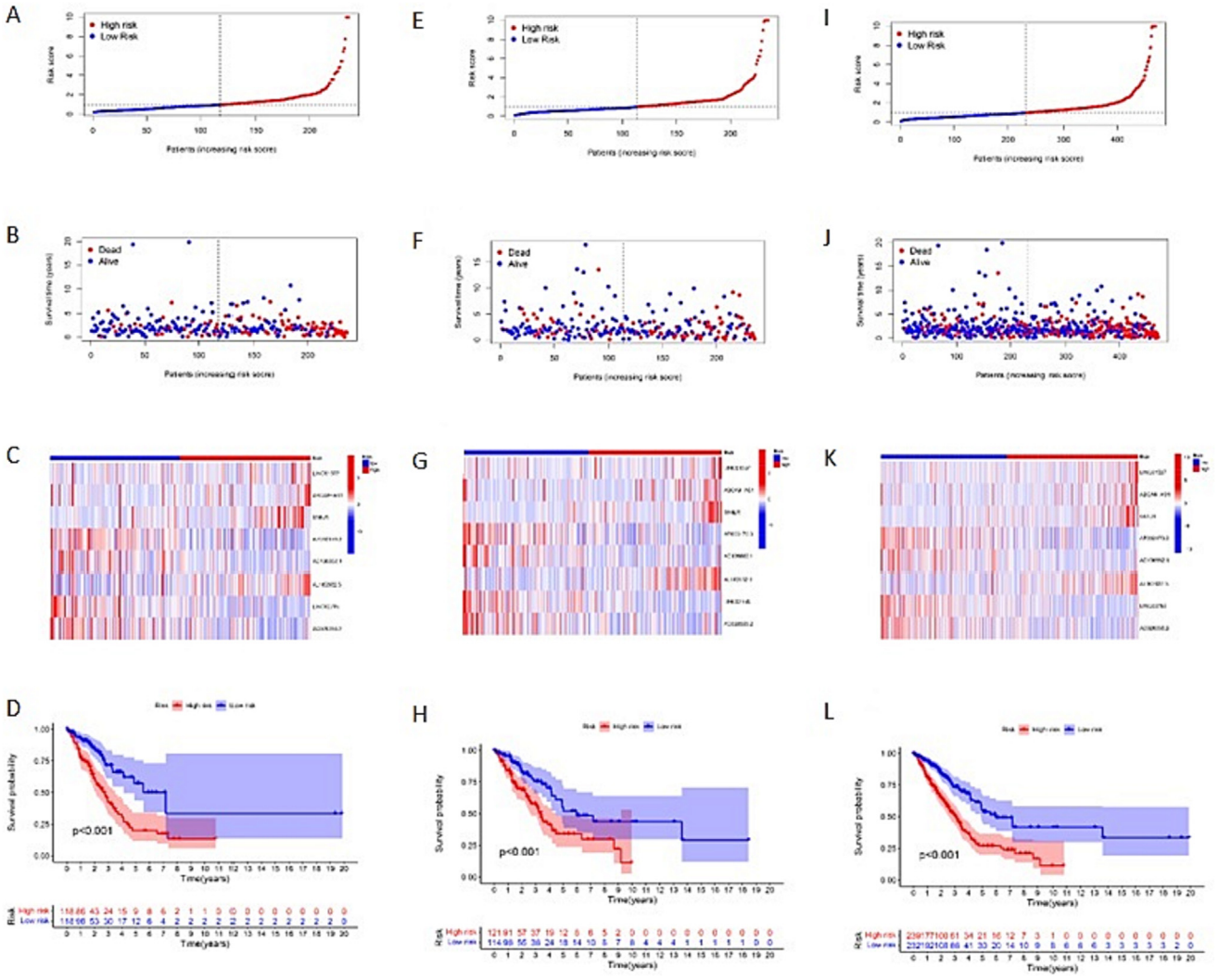

Fig. 4. Evaluation of SARS-CoV-2-associated lncRNA model in the training set (A-D), test set (E-H), and entire set (I-L). (A, E, I) Distribution of the RS of each sample. (B, F, J) A scatter plot of the survival status of each sample. (C, G, K) Heat map showing the distribution of eight SARS-CoV-2-associated lncRNAs in the two groups. (D, H, L) Kaplan-Meier curves of OS in the two groups grouped by the SARS-CoV-2-associated lncRNA model.

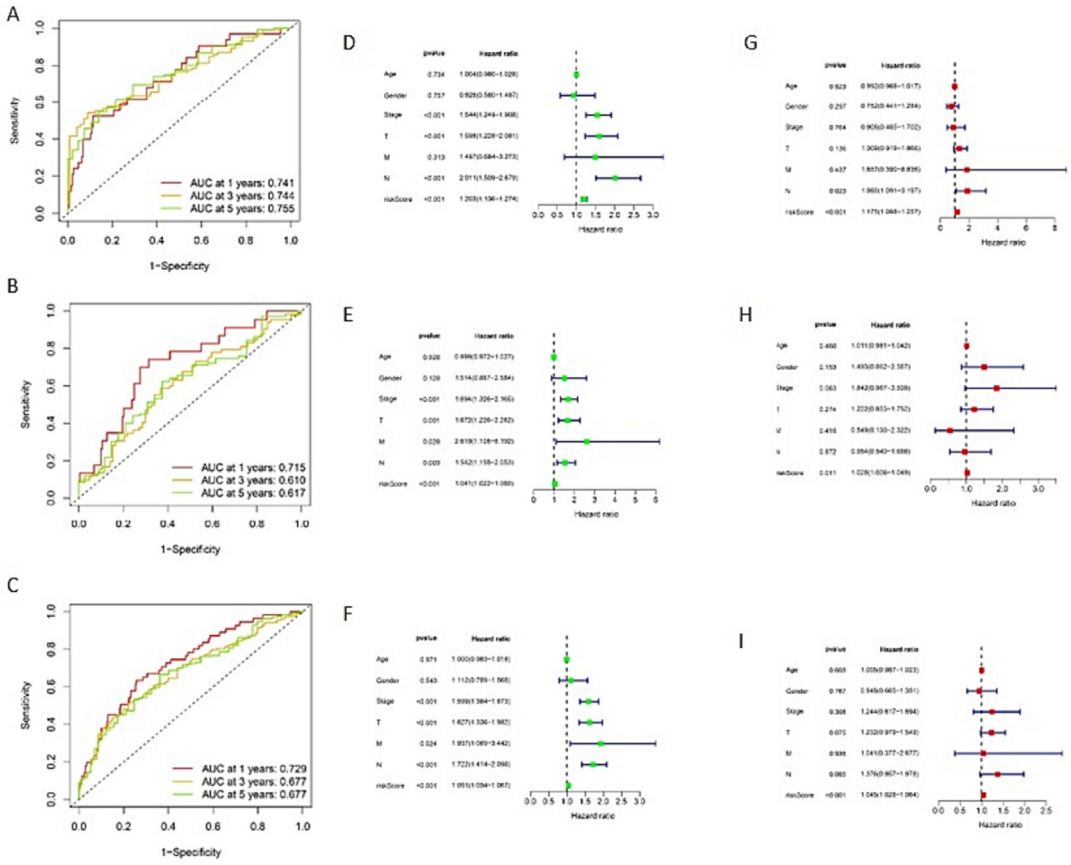

Fig. 5. Evaluation of SARS-CoV-2-associated lncRNA model in the training set (A, D, G), test set (B, E, H), and entire set (C, F, I). (A-C) Time-dependent ROC curves of one-, three-, and five-year OS. (G-I) Univariate and (D-F) multivariate Cox independent prognostic analyses combining clinical characteristics.

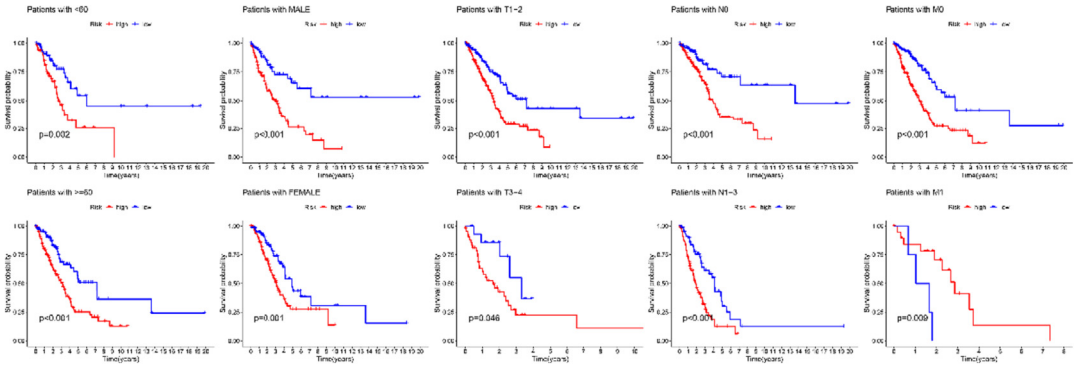

Fig. 6. A subgroup analysis of Kaplan-Meier survival was performed in all LUAD patients according to the SARS-CoV-2-associated lncRNA characteristics stratified by clinical features.

lncRNAs prognostic risk model could independently predict the prognosis of LUAD patients and effectively distinguish different risk groups.

3.5. Establishment of a new predictive nomogram

A nomogram for clinical prediction of survival was constructed based on the SARS-CoV-2-associated lncRNAs prognostic risk model. Significant clinical factors, including sex, age, T stage, RS, and tumor stage, were selected from the univariate independent prognostic analysis. The one-, three-, and five-year nomograms of LUAD patients were generated by stages (Fig. 8A). Subsequently, calibration curves were plotted for one-, three-, and five-year nomograms, with the x-axis representing the probabilities predicted by the nomograms and the Y-axis representing the actual survival probabilities of LUAD samples (Fig. 8B). The calibration plots revealed that predicted curves for one-, three-, and five-year periods are close to actual curves, indicating that the nomograms estimate mortality close to the actual mortality.

3.6. Analysis of signaling pathways and immune-related functions of SARS-CoV-2-associated lncRNAs prognostic risk model

In this study, the two risk groups' data of SARS-CoV-2-associated lncRNAs were input into GSEA to further analyze the functional pathways. The results identified that the top 5 enriched

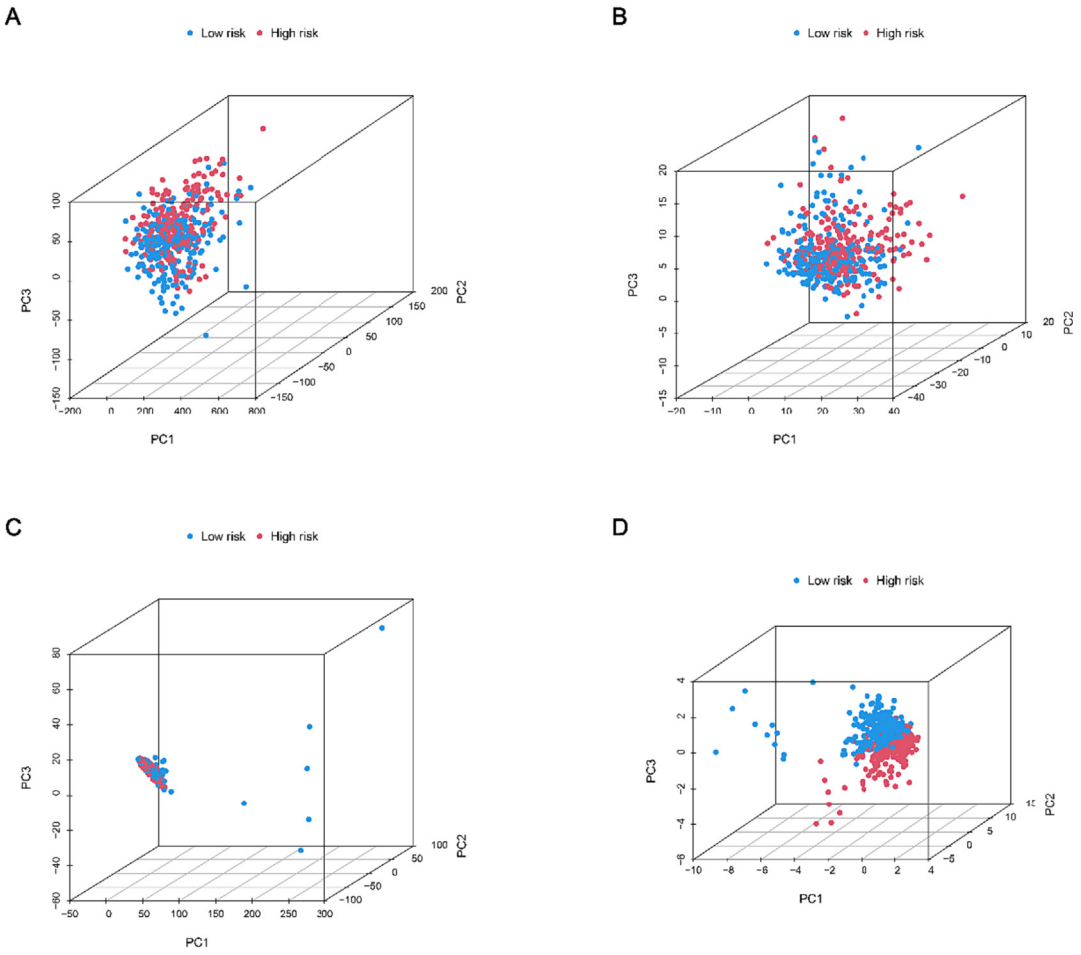

Fig. 7. PCA of low-risk and high-risk groups based on (A) genome-wide, (B) SARS-CoV-2-associated genes, (C) SARS-CoV-2-associated lncRNA, and (D) SARS-CoV-2-associated lncRNA prognostic risk model.

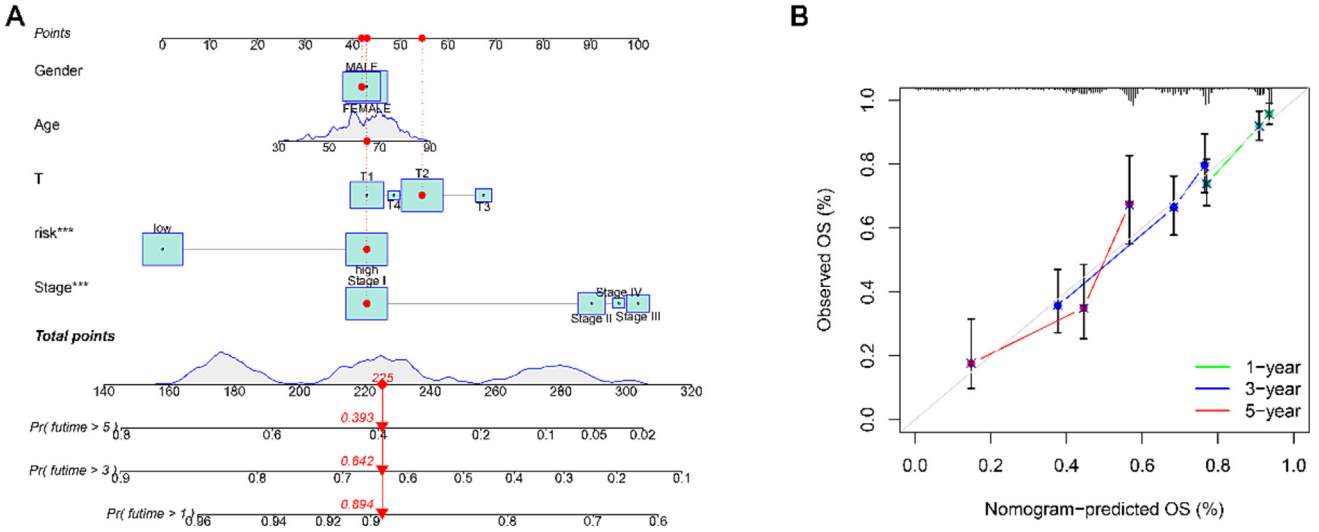

Fig. 8. A clinical prognostic nomogram is used to predict survival. The nomogram (A) and a calibration curve (B) were constructed to predict the 1,3,5-year survival rate of LUAD patients.

pathways were alzheimers disease, huntingtons disease, n glycan biosynthesis, protein export, pyrimidine metabolism in high-risk group, and asthma, autoimmune thyroid disease, leishmania infection, hematopoietic cell lineage, intestinal immune network for iga production in low-risk group (Fig. S1A). These could be the pathways related to SARS-CoV-2-associated lncRNAs, which may provide a basis for the development of future targeted therapy for LUAD patients.

To assess the correlation between RS and tumor immune cell infiltration, immune cells associated with the high-risk group derived using different quantification algorithms were displayed with bubble plots. The results demonstrated that progenitor lymphoid and T cell CD4 + Th2 were highly correlated with risk scores in XCELL, T cell $CD4^+$ (non-regulatory) and uncharacterized cells in QUANTISEQ, and uncharacterized cells in EPIC (Fig. S1B).

Next, we analyzed the association between the SARS-CoV-2-associated lncRNAs expression and the tumor microenvironment in both groups. "ESTIMATE" package of R software was used to compare the differences in the stromal, immune, and ESTIMATE scores between the two groups. The results revealed higher values of immune, stromal, and ESTIMATES scores in the low-risk group (Fig. S1C-E). This indicates the presence of greater tumor purity in the high-risk group. Furthermore, the link between the expression levels of the eight immune checkpoints in the two risk groups stratified by the SARS-CoV-2-associated lncRNA model was studied. The expression of the eight immune checkpoint genes was higher in the low-risk group as compared to that of the high-risk group. These results suggest that SARS-CoV-2-associated lncRNAs are potential biomarkers for immunosuppressive therapy and can be used to personalize therapy for patients with immune checkpoint blockade therapy (Fig. S2A-H).

3.7. Sensitivity analysis of risk models in the treatment of LUAD

IC50 is an internationally recognized indicator of the antitumor activity of drugs. IC50 values of chemotherapeutic drugs and targeted drugs were analyzed in high- and low-risk groups. IC50 values of docetaxel, gemcitabine, erlotinib, and paclitaxel were lower in high-risk group, suggesting higher sensitivity of the high-risk group to the above agents (Fig. S2I-N). No significant difference was observed in terms of cisplatin and gefitinib between the two groups (Fig. S2I-N).

4. Discussion

According to statistics, on average, every year about 25% of cancer patients die of lung cancer. There are many pathological types of lung cancer, among which lung adenocarcinoma is one of the most common subtypes. The COVID-19 epidemic has been spreading worldwide since 2020 with rapid variation and strong infectivity [17]. Cancer patients are more susceptible to SARS-CoV-2 infection. The systemic inflammatory response is one of the common underlying mechanisms of cancer progression and the exacerbation of coronavirus. SARS-CoV-2 induces the secretion of a large number of cytokines abnormally, and ACE2 has been reported to be a key factor in the transmission of SARS-CoV-2 within the human population [18,19]. Other studies found that tumor cells can also secrete ACE2 abnormally, such as LUAD, and digestive tract tumors, and are related to tumor prognosis and immune infiltration [20,21].

Growing evidence has indicated the crucial role of lncRNAs in the biological process of tumorigenesis and development. Abnormities in the expression of lncRNAs in malignant tumors could be used as molecular markers for prognosis, diagnosis, and targeted therapy [22]. Therefore, the study aimed to construct a prognostic risk model based on SARS-CoV-2-associated lncRNAs, which can provide the basis for individualized treatment of lung adenocarcinoma in the future.

In this study, a series of bioinformatics methods were used to analyze the correlation between lncRNAs and SARS-CoV-2-associated genes. The SARS-CoV-2 lncRNAs associated with the prognosis of LUAD were obtained using the univariate COX regression and Lasson regression analyses. Subsequently, multivariate COX regression analysis was used to establish and validate the optimal 8 SARS-CoV-2-associated LncRNAs model. Numerous studies have indicated the role of LINC01537 in the biological process of malignant tumors such as lung cancer, hepatic-biliary-pancreatic, gastric cancer, and so on [23,24]. LINC01537 has previously been shown to be overexpressed in gastric cancer and has also been reported to regulate the proliferation, invasion, and metastasis of cancer cells, both in vivo and in vitro [25]. ABCA9-AS1 was first reported to be associated with the regulatory mechanism of lncRNAs in the initiation and development of epithelial-mesenchymal transition in calcium oxalate-induced crystalline kidney injury [26]. A study found that ABCA9-AS1 expression was up-regulated 48 hours after calcium oxalate stimulation in HK-2 cells [27]. But ABCA9-AS1 has not been reported in cancer. SMILR has been extensively studied in the fields of vascular biology and disease, such as arteriosclerosis, pulmonary hypertension, and thoracic aortic aneurysm [28,29,30,31,32,33,34,35]. It was first mentioned in a study of neuroendocrine tumors, but its specific pathogenesis in cancer has not been clarified [36]. AC026355.2 has been deeply studied in LUAD. Whether AC026355.2 promotes tumor development through SARS-CoV-2-associated lncRNAs is unclear. The other four SARS-CoV-2-associated lncRNAs have not been reported in cancer thus far therefore, further studies are required to understand their significance.

A prognostic model for LUAD developed based on 8 SARS-CoV-2-associated lncRNAs showed significantly better survival in low-risk group than high-risk group as per survival analysis of LUAD samples. As demonstrated in the survival status and risk score chart, the mortality increases with an increase in the risk value. In addition, univariate and multivariate COX regression analyses as well as PCA verified the independence and accuracy of the SARS-CoV-2-associated lncRNAs model in predicting the prognosis of patients with LUAD. According to the ROC curve, Nomogram, and calibration chart were developed for one-, three- and five-year survival periods. The model demonstrated high accuracy in the prediction of the prognosis of LUAD individuals, which in turn provides potential direction for clinical research.

Enrichment analysis showed that protein output, pyrimidine metabolism, n-glycan biosynthesis, Alzheimer's disease, and Huntington's disease were significantly enriched in the high-risk group, which could be associated with the progression of LUAD. Previous studies have indicated the role of pyrimidine metabolism and n-glycan biosynthesis in the prognosis and pathogenesis of LUAD [37,38]. Based on the ESTIMATE analysis, three tumor microenvironment (TMI) scores were found to be significantly higher in low-risk group than in high-risk group. Several studies have shown that a major stromal component in the tumor microenvironment not only promotes tumor growth and metastasis but also influences anti-tumor immune responses, resulting in a poor prognosis [39,40] Our findings are consistent with previous results that higher TMI scores and lower tumor purity are associated with poor prognosis of the tumor [41].

Immune checkpoint inhibitor (ICI) is a crucial method used in tumor immunotherapy which targets immune checkpoint molecules providing inhibitory signals to T cells. It has been shown to improve survival in patients with refractory tumors. To explore the potential significance of the SARS-CoV-2-associated lncRNAs prognostic risk model in the immunotherapy of LUAD patients, we further analyzed the expression levels of 8 immune checkpoint molecules in high- and low-risk groups using this model. Expression levels of all 8 immune checkpoint molecules were found to be lower in high-risk group as compared with low-risk group, suggesting that immune-targeted therapy could be less effective in high-risk patients. This demonstrates that the 8 SARS-CoV-2-associated lncRNAs could be used as potential biomarkers to aid patient selection and decision-making for ICI-based therapies.

IC50 is recognized by WHO as an indicator of the antitumor activity of drugs. We further compared the difference in IC50 values for targeted and chemotherapeutic drugs between the high- and low-risk groups. IC50 values for docetaxel, erlotinib, gemcitabine, and paclitaxel were found to be significantly higher in low-risk group than high-risk group, while the IC50 values for Cisplatin and gefitinib were not significantly different between the two groups. This indicates that patients in high-risk group could be more responsive to anti-tumor treatment with docetaxel, erlotinib, gemcitabine, and paclitaxel. The functional analysis results revealed that the SARS-CoV-2-associated lncRNAs model could be used to predict the sensitivity of patients diagnosed with LUAD to anti-tumor drugs.

Study also has certain limitations such as: (1) The imbalance of sample size as the study relied solely on data retrieved from the TCGA database, and there may be an unequal distribution of tumor samples and normal tissue samples, which could introduce bias and affect the generalizability of the findings. (2) The study focused on the association between SARS-CoV-2-associated lncRNAs and LUAD prognosis, but did not consider potential confounding factors such as comorbidities, treatment history, or other clinical variables that could impact patient outcomes. (3) The findings were solely based on computational bioinformatics analysis of publicly available data. Experimental validation, such as in vitro or in vivo studies, were not conducted to confirm the functional relevance or biological effects of the identified lncRNAs. Further validation and functional studies are warranted to elucidate the underlying mechanisms and validate the clinical utility of the identified prognostic risk model. To establish a more concrete association between the identified lncRNAs and SARS-CoV-2, further investigations such as experiments using SARS-CoV-2-infected samples, functional assays, or validation in relevant COVID-19 datasets would be necessary. These additional steps would help to determine the specific roles and functional significance of these lncRNAs in the context of SARS-CoV-2 infection.

5. Conclusions

Our study investigated the role of SARS-CoV-2-associated lncRNAs in the prognosis of patients with LUAD and developed a prognostic risk model based on these lncRNAs, which were proved with good predictive performance and may aid in clinical decision-making and patient management. The differences in the high- and low-risk groups, grouped based on this model, in immune function, semi-inhibitory concentration (IC50), and immune checkpoints, suggested the potential implications of immunotherapy and personalized treatment strategies.

Author contributions

- Study conception and design: Z Xie, Y Chen.
- Data collection: Z Xie, Y Chen.
- Analysis and interpretation of results: Q Zhou, T Yuan, Z Xie, Y Chen.
- Draft manuscript preparation: Q Zhou, T Yuan.
- Revision of the results and approval of the final version of the manuscript: Q Zhou, T Yuan, Z Xie, Y Chen.

Financial support

Hunan Provincial Natural Science Foundation (Provincial and Municipal Joint Fund) (#2022JJ50105).

Conflicts of interest

The authors declare no competing interests.

Data availability

The datasets generated and/or analyzed during the current study are available in the [https://portal.gdc.cancer.gov/].

Supplementary material

https://doi.org/10.1016/j.ejbt.2023.10.001.

References

[1] Ettinger DS, Wood DE, Aisner D, et al. NCCN guidelines insights: Non-small cell lung cancer, Version 2.2021. J Natl Compr Canc Netw 2021;19(3):254–66. https://doi.org/10.6004/jnccn.2021.0013. PMid: 33668021.
[2] Hutchinson BD, Shroff GS, Truong MT, et al. Spectrum of lung adenocarcinoma. Semin Ultrasound CT MRI 2019;40(3):255–64. https://doi.org/10.1053/j.sult.2018.11.009. PMid: 31200873.
[3] Succony L, Rassl DM, Barker AP, et al. Adenocarcinoma spectrum lesions of the lung: Detection, pathology and treatment strategies. Cancer Treat Rev 2021;99:102237. https://doi.org/10.1016/j.ctrv.2021.102237. PMid: 34182217.
[4] Huang C, Wang Y, Li X, et al. Clinical features of patients infected with 2019 novel coronavirus in Wuhan. China Lancet 2020;395(10223):497–506. https://doi.org/10.1016/S0140-6736(20)30183-5. PMid: 31986264.
[5] Lu R, Zhao X, Li J, et al. Genomic characterisation and epidemiology of 2019 novel coronavirus: Implications for virus origins and receptor binding. Lancet 2020;395(10224):565–74. https://doi.org/10.1016/S0140-6736(20)30251-8. PMid: 32007145.
[6] Lai CC, Shih TP, Ko WC, et al. Severe acute respiratory syndrome coronavirus 2 (SARS-CoV-2) and coronavirus disease-2019 (COVID-19): The epidemic and the challenges. Int J Antimicrob Agents 2020;55(3):105924. https://doi.org/10.1016/j.ijantimicag.2020.105924. PMid: 32081636.
[7] Malkani N, Rashid MU. SARS-COV-2 infection and lung tumor microenvironment. Mol Biol Rep 2021;48(2):1925–34. https://doi.org/10.1007/s11033-021-06149-8. PMid: 33486674.
[8] Moujaess E, Kourie HR, Ghosn M. Cancer patients and research during COVID-19 pandemic: A systematic review of current evidence. Crit Rev Oncol Hematol 2020;150:102972. https://doi.org/10.1016/j.critrevonc.2020.102972. PMid: 32344317.
[9] Tortorici MA, Veesler D. Structural insights into coronavirus entry. In: FA Rey editor, Complementary strategies to understand virus structure and function. Adv Virus Res. 2019;105(Chapter 4):93–116. https://doi.org/10.1016/bs.aivir.2019.08.002. PMid: 31522710.
[10] Wan Y, Shang J, Graham R, et al. Receptor recognition by the novel coronavirus from Wuhan: An analysis based on decade-long structural studies of SARS coronavirus. J Virol 2020;94(7):e00127–e220. https://doi.org/10.1128/JVI.00127-20. PMid: 31996437.
[11] Mercer TR, Dinger ME, Mattick JS. Long non-coding RNAs: Insights into functions. Nat Rev Genet 2009;10(3):155–9. https://doi.org/10.1038/nrg2521. PMid: 19188922.
[12] Gupta RA, Shah N, Wang KC, et al. Long non-coding RNA *HOTAIR* reprograms chromatin state to promote cancer metastasis. Nature 2010;464(7291):1071–6. https://doi.org/10.1038/nature08975. PMid: 20393566.
[13] Therneau, T. Survival: A package for survival analysis in R. R package version 3.2-13 [cited 2022 June 13]; 2021. Available from: https://CRAN.R-project.org/package=survival.
[14] Friedman J, Hastie T, Tibshirani R. et al. glmnet: Lasso and Elastic-Net Regularized Generalized Linear Models. R package version 4.1-2 [cited 2022 June 17]. Available from: https://CRAN.R-project.org/package=glmnet.
[15] Pérez Fernández S, Martínez Camblor P, Filzmoser P, et al. nsROC: An R package for non-standard ROC curve analysis. The R Journal 2018;10(2):55–77. https://doi.org/10.32614/RJ-2018-043.
[16] Harrell Jr FE. rms: Regression Modeling Strategies. R package version 6.2-0; 2020 [cited 2022 June 21]. Available from: https://CRAN.R-project.org/package=rms.
[17] Jin YH, Cai L, Cheng ZS, et al. A rapid advice guideline for the diagnosis and treatment of 2019 novel coronavirus (2019-nCoV) infected pneumonia (standard version). Mil Med Res 2020;7(1):4. https://doi.org/10.1186/s40779-020-0233-6. PMid: 32029004.
[18] Li Y, Zhou W, Yang L, et al. Physiological and pathological regulation of ACE2, the SARS-CoV-2 receptor. Pharmacol Res 2020;157:104833. https://doi.org/10.1016/j.phrs.2020.104833. PMid: 32302706.
[19] Ashraf UM, Abokor AA, Edwards JM, et al. SARS-CoV-2, ACE2 expression, and systemic organ invasion. Physiol Genomics 2021;53(2):51–60. https://doi.org/10.1152/physiolgenomics.00087.2020. PMid: 33275540.

[20] Chen L, Liu Y, Wu J, et al. Lung adenocarcinoma patients have higher risk of SARS-CoV-2 infection. Aging 2021;13(2):1620–32. https://doi.org/10.18632/aging.202375. PMid: 33429366.
[21] He C, Hua X, Sun S, et al. Integrated bioinformatic analysis of SARS-CoV-2 infection related genes ACE2, BSG and TMPRSS2 in aerodigestive cancers. J Inflam Res 2021;14:791–802. https://doi.org/10.2147/JIR.S300127. PMid: 33732005.
[22] Peng Z, Liu C, Wu M. New insights into long noncoding RNAs and their roles in glioma. Mol Cancer 2018;17(1):61. https://doi.org/10.1186/s12943-018-0812-2. PMid: 29458374.
[23] Zhang J, Xiao J, Wang Y, et al. A universal co-expression gene network and prognostic model for hepatic-biliary-pancreatic cancers identified by integrative analyses. FEBS Open Bio 2022;12(11):2006–24. https://doi.org/10.1002/2211-5463.13478. PMid: 36054420.
[24] Ye L, Jin W. Identification of lncRNA-associated competing endogenous RNA networks for occurrence and prognosis of gastric carcinoma. J Clin Lab Anal 2021;35(12):e24028. https://doi.org/10.1002/jcla.24028. PMid: 34704289.
[25] Gong W, Yang L, Wang Y, et al. Analysis of survival-related lncRNA landscape identifies a role for LINC01537 in energy metabolism and lung cancer progression. Int J Mol Sci 2019;20(15):3713. https://doi.org/10.3390/ijms20153713. PMid: 31374807.
[26] Zhong GY, Tan JN, Huang J, et al. LncRNA LINC01537 promotes gastric cancer metastasis and tumorigenesis by stabilizing RIPK4 to activate NF-κB signaling. Cancers 2022;14(21):5237. https://doi.org/10.3390/cancers14215237. PMid: 36358656.
[27] Hu H, Zhang J, Li Y, et al. LncRNA SPANXA2-OT1 participates in the occurrence and development of EMT in calcium oxalate crystal-induced kidney injury by adsorbing miR-204 and up-regulating Smad5. Front Med 2021;8:719980. https://doi.org/10.3389/fmed.2021.719980. PMid: 34646842.
[28] Jaé N, Heumüller AW, Fouani Y, et al. Long non-coding RNAs in vascular biology and disease. Vasc Pharmacol 2019;114:13–22. https://doi.org/10.1016/j.vph.2018.03.003. PMid: 30910127.
[29] Li H, Pan Z, Chen Q, et al. SMILR aggravates the progression of atherosclerosis by sponging miR-10b-3p to regulate KLF5 expression. Inflammation 2020;43(5):1620–33. https://doi.org/10.1007/s10753-020-01237-6. PMid: 32367412.
[30] Lei S, Peng F, Li ML, et al. LncRNA-SMILR modulates RhoA/ROCK signaling by targeting miR-141 to regulate vascular remodeling in pulmonary arterial hypertension. Am J Physiol Heart Circ Physiol 2020;319(2):. https://doi.org/10.1152/ajpheart.00717.2019. PMid: 32559140H377-91-h391.
[31] Byun S, Affolter KE, Snow AK, et al. Differential methylation of G-protein coupled receptor signaling genes in gastrointestinal neuroendocrine tumors. Sci Rep 2021;11(1):12303. https://doi.org/10.1038/s41598-021-91934-5. PMid: 34112938.
[32] Lu Y, Luo X, Wang Q, et al. A novel necroptosis-related lncRNA signature predicts the prognosis of lung adenocarcinoma. Front Genet 2022;13:862741. https://doi.org/10.3389/fgene.2022.862741. PMid: 35368663.
[33] He C, Yin H, Zheng J, et al. Identification of immune-associated lncRNAs as a prognostic marker for lung adenocarcinoma. Transl Cancer Res 2021;10(2):998–1012. https://doi.org/10.21037/tcr-20-2827. PMid: 35116427.
[34] Gong Z, Li Q, Li J, et al. A novel signature based on autophagy-related lncRNA for prognostic prediction and candidate drugs for lung adenocarcinoma. Transl Cancer Res 2022;11(1):14–28. https://doi.org/10.21037/tcr-21-1554. PMid: 35261881.
[35] Liu J, Liu Q, Shen H, et al. Identification and validation of a three pyroptosis-related lncRNA signature for prognosis prediction in lung adenocarcinoma. Front Genet 2022;13:838624. https://doi.org/10.3389/fgene.2022.838624. PMid: 35928454.
[36] Wang H, Wang X, Xu L, et al. High expression levels of pyrimidine metabolic rate-limiting enzymes are adverse prognostic factors in lung adenocarcinoma: A study based on the Cancer Genome Atlas and Gene Expression Omnibus datasets. Purinergic Signal 2020;16(3):347–66. https://doi.org/10.1007/s11302-020-09711-4. PMid: 32638267.
[37] Lattová E, Skřičková J, Hausnerová J, et al. *N*-Glycan profiling of lung adenocarcinoma in patients at different stages of disease. Mod Pathol 2020;33(6):1146–56. https://doi.org/10.1038/s41379-019-0441-3. PMid: 31907375.
[38] Turley SJ, Cremasco V, Astarita JL. Immunological hallmarks of stromal cells in the tumour microenvironment. Nat Rev Immunol 2015;15(11):669–82. https://doi.org/10.1038/nri3902. PMid: 26471778.
[39] Quail DF, Joyce JA. Microenvironmental regulation of tumor progression and metastasis. Nat Med 2013;19(11):1423–37. https://doi.org/10.1038/nm.3394. PMid: 24202395.
[40] Zhang C, Cheng W, Ren X, et al. Tumor purity as an underlying key factor in glioma. Clin Cancer Res 2017;23(20):6279–91. https://doi.org/10.1158/1078-0432.CCR-16-2598. PMid: 28754819.
[41] Zhao Z, Zhao D, Xia J, et al. Immunoscore predicts survival in early-stage lung adenocarcinoma patients. Front Oncol 2020;10:691. https://doi.org/10.3389/fonc.2020.00691. PMid: 32457841.